International Journal of Neural Systems, Vol. 24, No. 5 (2014) 1440002 (19 pages)

DOI: 10.1142/S0129065714400024

World Scientific
www.worldscientific.com

SIMULATING VERTICAL AND HORIZONTAL INHIBITION WITH SHORT-TERM DYNAMICS IN A MULTI-COLUMN MULTI-LAYER MODEL OF NEOCORTEX

BEATA STRACK
Department of Computer Science
Virginia Commonwealth University
Richmond, VA, USA
strackb@vcu.edu

KIMBERLE M. JACOBS
Department of Anatomy and Neurobiology
Virginia Commonwealth University
Richmond, VA, USA
kmjacobs@vcu.edu

KRZYSZTOF J. CIOS*
Department of Computer Science
Virginia Commonwealth University
Richmond, VA, USA

IITiS Polish Academy of Sciences, Poland
kcios@vcu.edu

Accepted 6 February 2014
Published Online 21 March 2014

The paper introduces a multi-layer multi-column model of the cortex that uses four different neuron types and short-term plasticity dynamics. It was designed with details of neuronal connectivity available in the literature and meets these conditions: (1) biologically accurate laminar and columnar flows of activity, (2) normal function of low-threshold spiking and fast spiking neurons, and (3) ability to generate different stages of epileptiform activity. With these characteristics the model allows for modeling lesioned or malformed cortex, i.e. examine properties of developmentally malformed cortex in which the balance between inhibitory neuron subtypes is disturbed.

Keywords: Multi-column multi-layer computational model; cortex; low-threshold spiking interneuron; fast-spiking interneuron.

1. Introduction

Both horizontal and columnar organizations of the neocortex are vital to its normal operations. Thalamic input to the cortex propagates in a specific laminar fashion, from layer IV to II/III, to V and VI.[1] The focality of this input is maintained by surrounding inhibition provided by basket cells that control horizontal spread of excitation.[1–3] This function of fast-spiking (FS) parvalbumin-containing basket cell inhibitory interneurons is in contrast to that of interneurons with a bipolar morphology[4–7] that allows for simultaneous inhibition in different layers but within a cortical column. Some bipolar interneurons contain somatostatin and have low threshold spiking (LTS) characteristics.[8,9] These two inhibitory cell types vary not only in their

*Corresponding author.

morphology, but also in their membrane properties, synaptic inputs, as well as their postsynaptic targets.[9–14] Because of this variation, changes in the effectiveness of LTS interneurons are expected to produce substantially different network effects than altering FS interneuron output. Under certain disease conditions, these two interneuron subtypes are in fact differentially affected.[15–20] Computational modification of these individual interneuron subtypes is a useful aid in understanding network alterations, particularly under disease conditions.

These two inhibitory subtypes have previously been modeled with different levels of detail, from very simple single compartment units,[21–24] to complex, multi-compartmental models.[25] Multiple models of cortical or thalamocortical circuits have been designed.[26–32] Functions of inhibitory interneurons are particularly emphasized in simulations of thalamocortical oscillations[33–37] but these models focus on inhibitory neurons in general, without distinguishing their subtypes. Different inhibitory subtypes are used in models of one or several layers within one column[25,38,39] or in large scale simulations where only global activity is the subject of analysis.[40–42] We are not aware of another cortical model with the two interneuron subtypes that preserves the multi-layer, multi-columnar structure that is crucial for analyzing a flow of activity in normal or malformed cortex.

We introduce here a computational multilayer model consisting of multiple cortical columns that employs the two inhibitory subtypes, along with a detailed description of neural connections within and between layers and columns. In addition, we use a synapse model that allows for modeling short-time plasticity. Parameters of connections, namely, the probability of a connection, maximal amplitude, half-width of postsynaptic potential (PSP), and latency to peak of PSP, differ according to the types and location of the interconnected neurons. This allows the resulting model to mimic details of neuronal connections with the use of a simple neuron model.

The development of such a cortex model is the first required step before generating and testing novel ideas about modulation of inhibitory subtypes in a developmentally malformed cortex.[43] Here we demonstrate that the model closely simulates a normal biological cortex.

The paper is organized as follows. Section 2 describes the structure and components of the cortical network model. Simulations and their results are discussed in Sec. 3, and we finish with conclusions.

2. Methodology

2.1. *Computational methods*

The artificial neural network described here is designed to be consistent with biological data regarding probabilities of connections, synapse strengths, PSP characteristics, and the number of neurons taken from published reports; we also used biological data from Jacobs Lab. In particular, the network is designed based mostly on data from studies of paired intracellular recordings between neuronal types.[44–47] Below we describe the most important components of the model.

Although there exist software packages that allow for network modeling,[48–51] we developed our own model to be able to easily modify the network structure, neuron model, connectivity patterns, and data collected from simulations.

2.1.1. *Topology of the network*

The network's topology accounts for spatial structure that consists of five columns and four layers, however, the number of column and layers can be easily extended. The model is consistent with the rat somatosensory cortex as follows:

- layer II/III — an association layer, consists of regular spiking (RS), LTS, and FS neurons
- layer IV — the input layer (thalamus projects into this layer), contains FS and LTS neurons, as well as spiny stellate (SS) neurons, modeled as RS neurons
- layer V — an output layer, consists not only of RS, LTS, and FS neurons but also of intrinsically bursting (IB) neurons
- layer VI — generates cortical outputs, consists of RS, FS and LTS neurons.

Numbers of every neural type in each layer are given in Table 1. Although not every aspect of cellular intrinsic properties and connectivity have been biologically examined for the mammalian neocortex, hundreds of studies have provided many

Table 1. Parameters used to generate neurons of different types and the distribution of neural types across layers.

	Parameters of the neuron model					Average number/percentage per layer			
	a	b	c	d	Max. firing freq. (Hz)	Layer II/III	Layer IV	Layer V	Layer VI
RS	0.02	0.2	[−65; −60]	[5; 8]	160	169/79	83/73	84/52	230/84
IB	0.02	0.2	[−55; −50]	[2; 4]	300	—	—	28/17	—
FS	[0.08; 0.1]	[0.175; 0.20]	−65	2	350	30/14	20/18	33/21	27/21
LTS	[0; 0.02]	[0.225; 0.25]	−65	2	212	16/7	11/9	15/10	15/5

required details.[3,52–58] Biologically verified information was used for specifying the relative number of neurons within different layers,[59] the total number of GABAergic neurons in specific layers,[60] the percentage of parvalbumin (PV)-stained neurons (FS),[60] the percentage of SS-immunostained neurons (LTS),[19,61] and the percentage of IB.[62,63] While there are additional types of GABAergic neurons,[4,8,9] these are in much smaller numbers and far less is known about their connectivity. Because PV- and SS-immunostained neurons make up the majority of GABAergic neurons in neocortex,[4] we restricted our model to these two inhibitory types. The total number of neurons that we use in one column is 761, which gives 3805 in the entire network. The model implements only about 5% of neurons in one column of the cortex but preserves the ratios of neuron types.

The spatial size of the network is consistent with the rat somatosensory cortex, namely, the distance between the centers of columns is 400 μm and the heights of the layers are: 400, 200, 600 and 600 μm, for layers II/III, IV, V and VI, respectively. When a neuron is placed in a particular layer, its spatial coordinates are chosen randomly with a uniform distribution in this layer.

The crucial aspect of building any network is the design of its topology. Connection between two neurons depends on the probability of a connection, amplitude, and shape of the PSPs. In our design we used published data, which is summarized in Table A.1 (Appendix A). Probabilities of connections vary not only with the types of neurons but also with their location within columns and layers. As a result, each cell type is connected in a unique way to the other cell types used in the model (Fig. 1). The probabilities define the spatial structure of the network, e.g. the degree distribution (the number of connections) or the shape of dendritic trees. Synapses between the neurons are characterized by their weights, which are determined using the data shown in Table A.1 (Appendix A). The strength of a connection was calculated as a weighted average of published results, with weights being inverses of the reported variances. This was done to take into account the fact that values reported in different reports had different standard deviations due to different sample sizes and methods used. The delays in connections (the time between the presynaptic neuron spikes and PSP is generated in the postsynaptic neuron) are based on the distance between neurons and averaged speed of signal propagation (4 m/s).

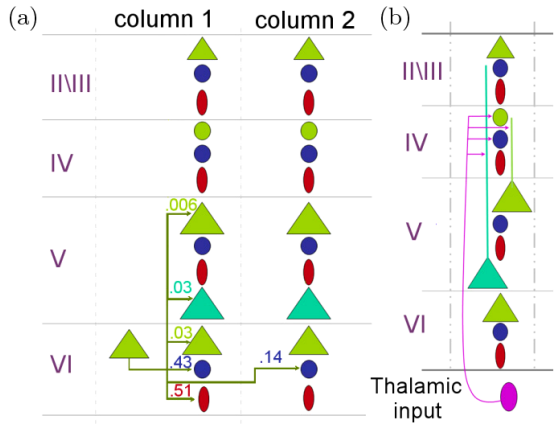

Fig. 1. (Color online) Example of connectivity. (a) RS neurons (light green triangle) in layer VI connect with different probabilities to IB neurons in layer V (dark green triangle), FS neurons (blue circle) in layer VI within the same and adjacent columns, LTS cells (red ellipse) in layer VI, and other RS cells in layers V and VI. Numbers shown reflect probability of connection to that cell type. (b) Connections of the thalamic input to one column.

The described details of connectivity allow the model to accurately mimic neuron connections

without actually modeling various compartments of neurons.

The thalamic input is modeled as a single cell connected to the selected cells within a single column and is provided to RS and FS neurons in layer IV, and to RS neurons in layer V. This is consistent with the processes that take place in rat somatosensory cortex. The resulting activity of the stimulated network is visualized in three ways: as a pattern of spikes, as an artificially generated local field potential (LFP), and as EEG. The spike pattern provides insight into how each neuron behaves and how single neuron responses contribute to the overall network activity. The computational EEG is generated by summation of the excitatory (EPSP) and the inhibitory (IPSP) postsynaptic potentials of all excitatory pyramidal cells in layers III and V, across all columns.[64] LFPs are calculated by adding the voltage of excitatory pyramidal cells in layers III and V in a single column.

2.1.2. *Neuron model*

A simple neuron model introduced by Izhikevich[65] is used in this work. It is a two-dimensional system of nonlinear ordinary equations in the form

$$\begin{cases} v' = 0.04v^2 + 5v + 140 - u + I, \\ u' = a(bv - u), \end{cases} \tag{1}$$

with the condition

$$\text{if } v > 30, \text{then } v = c, u = u + d, \tag{2}$$

where v represents the membrane potential of the neuron and u is a membrane recovery variable (both are functions of time), a, b, c and d are dimensionless parameters, and I is the value of the input to the neuron. The membrane potential v has an mV scale and the time ms scale. Depending on the values of parameters in Eqs. (1) and (2) this model mimics the spike patterns of different types of neurons[22] (Fig. 2).

Parameters used for generating the four types of neurons are shown in Table 1 and are based on previously published values.[65] To achieve heterogeneity of the neurons' dynamics some parameters were fixed and some generated from a uniform distribution on a given interval. These equations are solved using Euler method. The stability of the equations and sensitivity of the parameters have been thoroughly analyzed.[65,66]

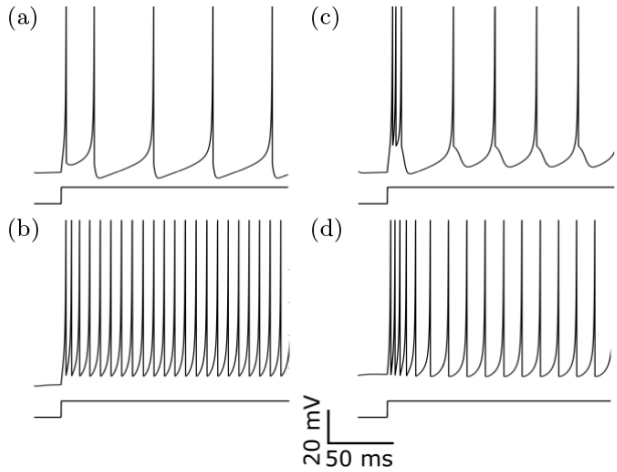

Fig. 2. Firing patterns of neurons of different type: (a) RS, (b) FS, (c) IB, and (d) LTS. The upper trace is the membrane potential of a neuron, the bottom trace is the stimulation.

The drawback of the above model is that it does not preserve neuronal maximal firing frequencies, which are especially important when one wants to account for frequency-dependent plasticity (short-term dynamics). A spike is generated always when the condition in (2) is satisfied. In case of a very powerful input (I in Eq. (1)), a neuron can spike arbitrarily fast. In our modification, the generation of action potential is prevented[67] if the time from the previous spike is shorter than that given by the maximal firing frequency (Table 1).

The value of input (I in Eq. (1)) represents all summed inputs coming to a neuron at a given time ($I = I(t)$), including PSPs or direct stimulation. In addition, white Gaussian noise is input to all neurons (independently) for two main reasons. First, to take into account that each neuron receives more connections than is modeled. Large sum of independent inputs can be approximated by the Gaussian distribution[68,69] (by the central limit theorem), so adding this noise is a way to simulate additional distant connections. Second, in the absence of any stimulus, biological networks exhibit spontaneous activity, which does not occur in artificial neural networks without adding any noise. Note that this is a bio-induced noise rather than noise resulting from measurement.

2.1.3. *Short-term plasticity and synapses*

Research reported in Refs. 70–77 indicates that nonlinear synapses are crucial to model and understand

the synchronous behavior of the network and various learning mechanisms. Therefore, the use of short-term plasticity (STP) is crucial for preserving important characteristic of a cortical model. There exist well-accepted models[77,78] of fast synaptic dynamics (STP), in particular the phenomenological model of Tsodyks[79] and the model of Abbot *et al.*[80] We use the first of these models because it accounts for different synapse behaviors reported in the literature, e.g. the short-term dynamics of neocortical synapses in layer VI.[47]

Short-time plasticity is an inherent dynamic of synapses that results in different responses of postsynaptic neurons for different temporal patterns of presynaptic spikes. Specifically, the postsynaptic response can be smaller (depression, e.g. in case of connections between layer II/III RS neurons[81]) or larger (facilitation, e.g. in case of connections from RS to LTS neurons in layer IV[44]) than the previous one.

The model of Tsodyks *et al.* consists of four equations:

$$\begin{cases} x' = \dfrac{z}{\tau_{\text{rec}}} - ux\delta(t - t_{\text{pres}}), \\ y' = -\dfrac{y}{\tau_I} + ux\delta(t - t_{\text{pres}}), \\ z' = \dfrac{y}{\tau_I} - \dfrac{z}{\tau_{\text{rec}}}, \\ u' = -\dfrac{u}{\tau_{\text{fac}}} + U(1-u)\delta(t - t_{\text{pres}}). \end{cases} \tag{3}$$

Here x, y, and z are the fractions of the synaptic resources in the recovered, active, and inactive states, respectively, t_{pres} is the time of the presynaptic spike, τ_I is the decay constant of the postsynaptic current, and τ_{rec} represents the recovery from the synaptic depression. The variable u is the fraction of the available resources used by the presynaptic spike. It increases with each presynaptic spike (this change is described by constant U) and decays accordingly to τ_{fac}.

These equations can be solved using exact integration technique, since between consecutive presynaptic spikes the system can be integrated linearly.[77]

The synapse behavior, e.g. the rate of facilitation or depression, varies not only with types of pre- and postsynaptic neurons but also with the layers where the neurons are located. We collected data from many published reports and chose the parameters in the model to reflect the reported behavior (Table A.1, Appendix A).

When the presynaptic neuron fires, the input to the postsynaptic neuron, the PSP is calculated as

$$\text{PSP}(t) = wy(t)C_{\text{norm}}(e^{-t/\tau_1} - e^{-t/\tau_2}), \tag{4}$$

where w is the weight of the connection, y is the fraction of active resources in the synapses calculated according to (3), τ_1 and τ_2 are decay constants, and C_{norm} is a normalizing constant. The values of τ_1, τ_2 and C_{norm} are chosen to match the shape of PSP reported in the literature for a particular connection (Table A.1, Appendix A).

The fact that various compartments of a neuron are not modeled is compensated here by the use of realistic: PSP shapes, timings, STP, and biologically measured strengths of connections. For example, the fact that LTS and FS neurons likely terminate along different parts of the somato-dendritic axis of pyramidal neurons is reflected in the network by different average amplitudes and half-widths of the generated IPSPs. In this way, without having a separate compartment, we are still able to model the difference in synaptic connectivity to the dendrites versus somata. Since our goal is to model modification of structure of the network (malformation) the use of a simple neuron model is sufficient for the purpose. Other researchers took the same approach in their modeling studies.[32,82,83]

2.2. *Biological methods*

Coronal slices through the somatosensory cortex of normal Sprague Dawley rats (P12–18) were prepared as previously described.[84] Field potential recordings were made with glass micropipettes (2–8 MΩ, 1 M NaCl) placed in superficial layers after online stimulation in deep layers, with a normal aCSF maintained at 34°C. The normal aCSF contained: (in mM) 126 NaCl, 3 KCl, 2 $MgCl_2$, 2 $CaCl_2$, 1.25 NaH_2PO_4, 10 glucose, and 26 $NaHCO_3$. Field potentials were amplified 1000x (AxoClamp 2B, Axon Instruments and FLA-01 amplifier, Cygnus Technologies) and digitized at 5 kHz with a Digidata 1322a (Axon Instruments) and recorded to hard drive with Clampex software (Axon Instruments). In order to generate a series of intensity responses, a threshold level of current was first determined by applying a 0.02 ms square pulse at a current level that produced a 0.2 mV peak negativity. The intensity was then

doubled four times to result in the following levels: 1X (threshold), 2X, 4X, 8X, and 16X. This series was then repeated, so that averages of three presentations could be made for each level. To demonstrate the loss of focal input as well as several types of epileptiform activity, for some experiments, bicuculline was applied in the slice bathing medium at concentrations of 0.01, 0.05 and 0.1 mM. In other experiments, the $MgCl_2$ was omitted from the aCSF in order to increase activation of NMDA receptors, and induce epileptiform activity.

3. Results and Discussion

We sought to validate that the designed model emulates the biology in terms of the following characteristics: (1) proper laminar flow of activity; (2) columnar organization with focality of inputs; (3) LTS neurons function properly in that enhancement of their input produces local 1 Hz oscillations, and reduction of their activity does not induce epileptiform activity, since they perform a primarily modulatory function, and also that blockade of their function does not cause spread of activity to adjacent columns, since their output is intracolumnar; (4) FS neurons function properly in that when they are blocked within one layer, activity in that layer spreads to adjacent columns, and when activity in these neurons is increased, a gamma rhythm is induced in the network; and finally, (5) that different stages of epileptiform activity (interictal-like and ictal-like) can be observed with either increasing levels of inhibitory blockade, or enhancement of NMDA receptors.

All simulations were performed on a network consisting of five columns with a time step of 0.1 ms, second column is the stimulated one, and Gaussian noise with zero mean and standard deviation of eight is added to the network unless indicated otherwise.

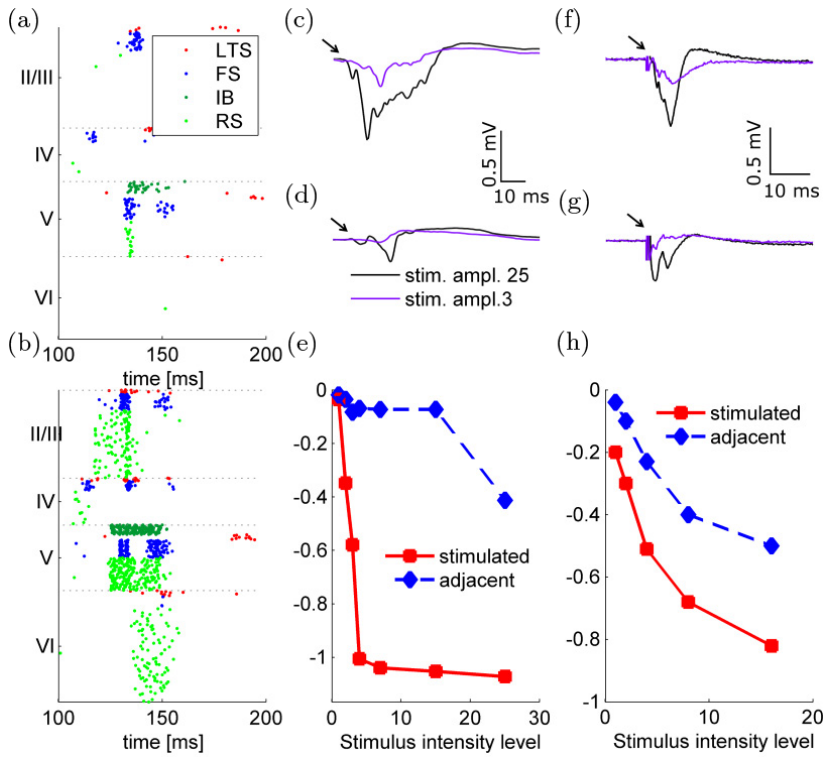

Fig. 3. Laminar and columnar flow of activity. (a–b) Spike pattern of activity in an adjacent (a) and the stimulated (b) columns as a response to stimulus with amplitude 3. (c–d) Computational Local Field Potentials (LFP) in the stimulated (c) and an adjacent (d) column as a response to two different levels of input. (f–g) Biological LFP in the stimulated column (f) and 0.5 mm away (g) as a response to two stimulus levels. (e–h) Peak negativity of LFP versus intensity of the stimulus. Computational results (e) were obtained by averaging 10 simulations. Column 2 was stimulated and the adjacent column is column 3.

3.1. *Laminar- and columnar-selective flow of activity*

In order to determine whether the proper laminar flow of activity occurs, we examined the timing of activity in different layers after thalamic input (activation of the selective thalamic cell, see Figs. 3(a) and 3(b)). Thalamic input to one column resulted in activity occurring first within layer IV, followed by activity in layer II/III, and then in layers V and VI, similar to what was shown biologically.[1] The time delay between stimulation and response was 4.44 (±0.17) ms in layer III and 0.9 (±0.23) ms in layer V (averaged over five experiments and calculated relative to response of layer IV); this is consistent with experimental results.[85]

In addition, the excitation occurs most prominently within the stimulated column. Although a weak excitation passes intracortically to the adjacent columns, it is damped by surrounding inhibition.

The generated LFPs also demonstrate and confirm this focal nature of the input. Namely, the computational LFP matches typical biological LFP in shape and in the increasing peak negativity while increasing stimulus intensity (Figs. 3(c)–3(e) and 3(h)). This is true for the stimulated column and the adjacent column. The simulations demonstrate that inhibition and excitation are properly balanced within- and between-columns.

3.2. *LTS neuronal function*

Depolarization of LTS neurons with a 1 Hz oscillatory input within one column results in synchronization of adjacent FS and pyramidal cells (Figs. 4(a) and 4(b)) that does not spread laterally into the adjacent columns. This is typical of what is observed biologically after application of metabotropic glutamate agonists.[86,87]

Since LTS neurons provide only modulatory inhibition, selective blockade of these cells would not be expected to result in a spread of activity within or between columns. Blockade of a neural cell was modeled by decreasing strengths (amplitudes) of all outgoing connections. When all LTS cells within two columns were blocked by 50%, as expected, there was little change in the computational LFP (Figs. 4(c) and 4(d)). Blockaded by 70% slightly decreased the latency of the evoked LFP in the blocked column,

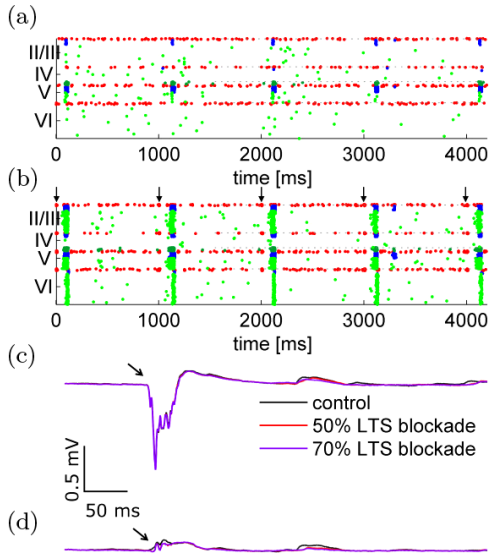

Fig. 4. (Color online) LTS neuronal function (a–b) LTS cells (red) were depolarized with input of 1 Hz frequency causing synchronization of RS (green) and FS (blue) neurons. The depolarizing current of value 5 was given to column 2 only (black arrows mark stimulation times) (b) and does not cause oscillations in adjacent columns (a). (c–d) Local Field Potentials (LFP) in the stimulated column 2 (c) and an adjacent column 3 (d) with different levels of LTS neuron blockade.

and increased the amplitude of a late component of the computational LFP (Figs. 4(c) and 4(d)). Little change was observed in the column adjacent to that stimulated even with 80% blockade of the LTS cells in both columns.

3.3. *FS neuronal function*

FS neurons provide inhibition that controls horizontal spread of excitation within the cortex.[1–3]

Simulation of increased strength of FS neurons within layer III showed that the computational LFP decreased in duration and amplitude (Fig. 5(g)). In addition, the response in the column adjacent to that stimulated was reduced, demonstrating an increased focality (Figs. 5(g) and 5(h)).

In contrast, when the strength of the FS neurons was selectively reduced, activity spread laterally within the cortex (Figs. 5(a) and 5(b)). Reduction or increase of the effectiveness of inhibitory synapses was achieved by decreasing or increasing weights of the synapses connecting inhibitory neurons to other cells.

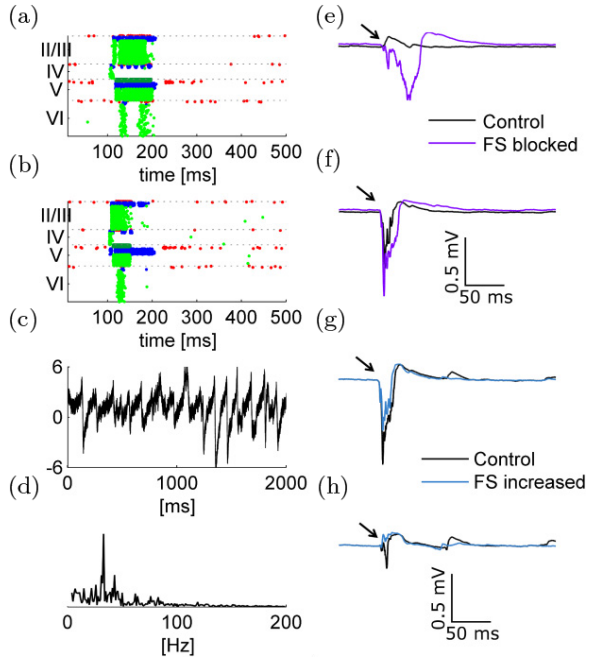

Fig. 5. (Color online) FS neuronal function. (a–b) Result of blockade of FS cells in layer III by 50%: activity in the stimulated (a) and an adjacent column (b). The amplitude of stimulus is 8. (e–f) LFP in the case of blockade (purple) is compared to the control case (black) both in stimulated (e) and an adjacent (f) column; (c–d) Gamma oscillations: EEG (c) and its Fourier transform (d) with a peak at 33 Hz. The depolarizing inputs were: 2–6 for RS cells, 3 for LTS and IB cells, and 4 for FS cells. (g–h) Results of strengthening FS cells to 200% their amplitude. LFP in the stimulated (g) and adjacent (h) column. The amplitude of stimulus is 25. Column 2 was stimulated and the adjacent column is column 3.

The cortical and thalamocortical oscillations in the gamma frequency (30–80 Hz) are well studied and described. They occur, for instance, in pharmacologically isolated networks of inhibitory interneurons and it has been shown that the interneurons that drive the gamma oscillations are the FS cells.[33,88]

Applying depolarizing currents, that effectively increase the function of FS cells, results in persistent gamma oscillations in the computationally generated EEG (Figs. 5(c) and 5(d)), which was calculated as the sum of all excitatory (EPSP) and inhibitory (IPSP) postsynaptic potentials of all excitatory cells in layers III and V, across all columns. The values of the current were: 2 mV to RS neurons in layer III and IV, 3 mV to all LTS and IB neurons and RS neurons in layer V, 6 mV to RS neurons in layer VI, and 4 mV to all FS neuron.

3.4. *Generation of interictal-like and ictal-like epileptiform activity*

Three sequential effects of decreasing levels of $GABA_A$ receptor blockade can be observed by looking at the evoked field potentials. First, the short latency evoked field increases in duration, reflecting a greater excitatory postsynaptic response. Second, longer but variable latency, polyphasic, all-or-none fields are evoked that are similar to interictal-like epileptiform activity. Third, repetitive sharp ictal-like waves are produced both spontaneously and in response to stimulation.

All three levels could be simulated with increasing reductions in all inhibitory synapses within the computational network (Figs. 6(b)–6(d)). The computational LFP generated under these conditions was similar to that produced biologically with application of the $GABA_A$ antagonist, bicuculline (Figs. 6(k)–6(m)). Under these conditions, a single stimulation pulse results in increased latency of the response, propagation across columns, and repetitive spiking. This gradual increase of activity with increase of inhibitory blockade is not achieved in network with neuron model that was not modified to adapt for maximal firing frequency (Figs. 6(f)–6(i)).

After 50 μM bicuculline was added to the bathing medium, stimulation at 8X produced repetitive ictal-like spiking during all three trials on 6 of 6 slices. Our computational model performed in a similar manner, producing ictal-like spikes in all 18 experiments (using different seeds) with a stimulation of 8 mV with 60% inhibition.

Epileptiform activity can also be induced in cortical slices acutely by activation of NMDA receptors with application of a bathing medium without the addition of $MgCl_2$.[89,90] Computationally, enhancing NMDA receptors was modeled by increasing the late component of the EPSC (Fig. 6(e)), since NMDA receptors account for the late part of the EPSP. Specifically, the value of τ_1 in Eq. (4) was increased by a factor of two.

4. Discussion

In this work, we presented a model of neocortex that allows for selective modulation of the powerful inhibition that maintains the boundaries on focal excitation separately from the form that provides simultaneous, modulatory inhibition to several layers

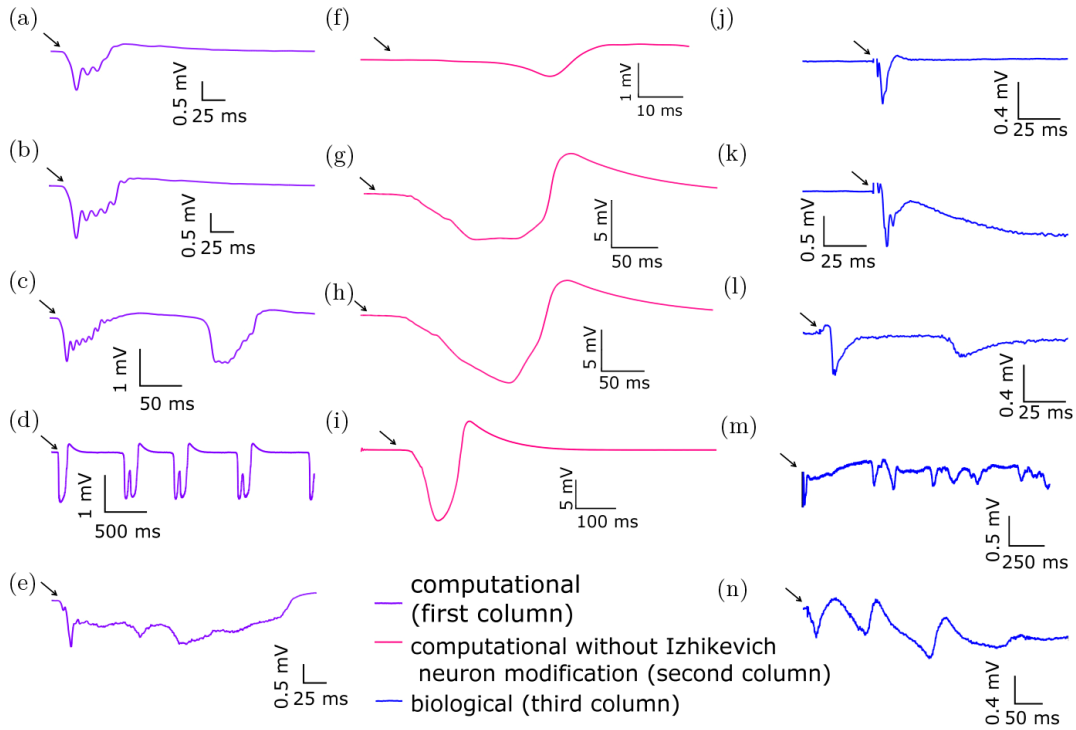

Fig. 6. Different stages of inhibitory blockade (a–e) Computational LFPs in the stimulated column at different conditions: control (a), increasing level of inhibitory blockade (b–d): 20%, 30%, and 90% respectively, and simulation of enhancement of NMDA receptors (e). Amplitude of input was 8 mV; (f–i) Computational LFPs for the stimulated columns in the network without modification of the neuron model with increasing level of inhibitory blockade 0 (control), 20%, 30%, and 90%, respectively. Amplitude of input was 3 mV; (j–n) Biologically measured LFP: control (j), increasing level of bicuculline (k–m), and enhancement of NMDA receptors (n).

within a column. A unique characteristic of this model is the multi-column, multi-layer construct. This allows for a better understanding of the processes that propagate across columns, as well as those that create inter-laminar synchrony. This model can specifically be used to probe questions about mechanisms underlying epileptiform activity induced in a malformed cortex.

When creating a computational model of neocortex, there are a number of questions that should be asked. First, how much detail is necessary in order to answer the specific questions proposed. High level models do not account for shapes of synaptic input, while more complex or 'detailed' models use multiple compartments for individual neurons and thus limit the size of the network that can be modeled within a reasonable computation time. In this work we used the best aspects of each model, allowing for simulation of different EPSC shapes, as necessary for instance to model NMDA inputs, but still having fast computing since neurons have only a single compartment. Since the main goal here is to understand how alteration of specific interneuron subtypes affects the development of propagating excitatory activity, multiple compartments are not necessary.

For example, the fact that LTS and FS neurons likely terminate along different parts of the somatodendritic axis of pyramidal neurons is reflected in the network by different average amplitudes and half-widths of the generated IPSPs. In this way, without having a separate compartment, we are still able to model the difference in synaptic connectivity to the dendrites versus somata.

Another critical question is which aspects of function are necessary to test in order to demonstrate that the computational model performs close to the biological network. Clearly the individual units from which the network is composed must be tested. We adopted the Izhikevich neuron model that has been used and tested in many studies to create neuronal subtypes with specific firing patterns. We have confirmed this unique firing pattern in

response to depolarization and added a crucial modification that prevents 'runaway' firing.[67] Without this modification, the neurons could fire at higher frequencies than those occurring biologically. In addition, in our network, we have confirmed two other critical aspects: (1) the correct form of STP on the synaptic inputs that the cell receives; and (2) the correct amplitude and probability of outputs to specific cell types, as shown by paired intracellular recordings. We have also demonstrated that their synaptic inputs and outputs produce the biologically demonstrated result. For LTS neurons, this includes a modulatory inhibitory output that spans the layers but remains confined within a column. For FS interneurons, this includes a powerful inhibition that is primarily within a single layer.

The goal of this work was to design a model that can be used, for instance, to determine connectivity patterns that generate epileptiform activity. Thus the other aspects of function necessary to test are those that contribute to patterns of activity under both conditions of normal network function and hyperexcitability, or seizure-like, function. Here we demonstrate that thalamic input produces the expected laminar and columnar pattern, namely, layer IV to II/III to V and VI, within a single column, without spread to other columns or activation of epileptiform activity. We have previously demonstrated other aspects of laminar and columnar flow of activity by modeling global and focal lesions,[91] namely, removal of specific layers either across all layers or within one column only. We have shown that with increasing inhibitory blockade the activity propagates across columns in both deep and superficial layers, but the threshold at which the propagation succeeds is lower for deep layers, as occurs in biological cortex.[92]

When conditions that produce epileptiform activity are applied to the model (blockade of inhibitory receptors, or increased function of NMDA receptors) the network undergoes the same pattern of changes that can be observed biologically. For instance, application of low levels of bicuculline to the bathing medium of a cortical slice block $GABA_A$ receptors and produce enhancement of the short latency evoked field potential.[93–95] This is also observed in our model with 20% inhibitory blockade. With increasing levels of bicuculline in the biological slice, interictal epileptiform activity occurs, the characteristics of which are a varied but typically long latency after the stimulus, variable form, and all-or-none event.[93–95] This means that the amplitude of the interictal event does not vary with stimulus intensity. In our model, we observe these same characteristics at 30% inhibitory blockade. Ultimately, with either strong $GABA_A$ blockade or removal of magnesium from the bathing solution, ictal-like events can be generated in cortical slices. These events typically have a sharp onset and are repetitive.[89,90] In our model we observe these same characteristics, at 90% level of inhibitory blockade, or enhancement of NMDA receptors equivalent to the removal of magnesium from the slice bath solution.

Computational models have commonly been used to understand different aspects of epileptiform activity.[31,96–101] For instance, the macroscopic approach, which involves modeling larger population of neurons instead of separate cells, provided many valuable insights, including modeling of EEG and the transition from interictal to ictal activity.[102,103] However, when the goal is to model the influence of connectivity, specific neural subtypes, or synaptic properties on epileptiform activity, network models are more appropriate. Although the network approach has been successfully combined with experimental studies,[25,104] there are several areas that have not been studied computationally, such as how malformation of the cortex affects the propagation of epileptiform activity.

The model described here was designed to enable simulation of focally malformed cortex under potentially epileptogenic conditions. We have shown elsewhere[91] that it generates results consistent with biological findings in conditions of either global or focal lesions, but cortical malformations involve not only loss of tissue but also several neuronal and connectional abnormalities in the area surrounding the malformation. It is currently not known what influence each of these changes has on the overall network function and our computational model can be used to provide valuable insights towards achieving this goal.

5. Conclusion

In the paper we introduced a multi-layer, multi-column cortex model, a network of spiking neurons,[105] that used four different neuron types with known firing patterns. Importantly, the model also

incorporated a short-term synaptic plasticity model to modify the synaptic strengths. The network was designed using all published (as of this writing) details of neuronal connectivity within and between the layers and columns. We have shown that the model mimicked biology in terms of: biologically accurate laminar and columnar flows of activity, normal function of LTS and FS neurons, and ability to generate different stages of epileptiform activity. Incorporation of these unique characteristics allowed for examining properties of cortex that were not previously modeled computationally. In particular, it was shown to be well suited for modeling propagation of activity in lesioned cortex.[91]

Appendix A

All used connection parameters in the network are shown in Table A.1. 'D' indicates depressing while 'F' indicates a facilitating synapse. T1, Trec, Tfac, and U are parameters of the STP model (see Eq. (3) in Sec. 2.1.3), T1 and T2 are parameters of PSP (see Eq. (4) in Sec. 2.1.3). The neuron type and location are coded as Ax, where A is the first letter of the neuron type, and x is the number representing a layer, e.g. R6 means RS neuron in layer VI.

Some information is available in the literature about cell types that project horizontally across the columns.[92,106,107] The actual values for probability and strength across the columns were based on a

Table A.1. Parameters of connections.

Presynaptic neuron	Possynaptic neuron	Columns away	Connections		Type	STP				PSP		References
			Probability	Strength		T1	Trec	TF	U	T1	T2	
R3	R3	0	0.16	0.49	D	3	100	10-6	0.30	0.5	20	55, 108–110
	F3	0	0.36	0.56	D	3	110	10-6	0.20	0.5	5	55, 109, 111
	L3	0	0.07	0.37	F	3	150	200	0.02	0.1	5	108, 109, 112–114
	R4	0	0.02	0.36						1	12	
	F4	0	0.01	0.05						0.1	5	
	L4	0	0.01	0.05						0.1	5	
	R5	0	0.3	1.13	D	3	100	10-6	0.40	1	18	115–118
	I5	0	0.3	1.13						1	18	
	F5	0	0.15	0.5						0.1	5	
	R3	1	0.08	0.343	D	3	100	10-6	0.30	0.5	20	
	F3	1	0.29	0.45	D	3	110	10-6	0.20	0.5	5	
	R3	2	0.04	0.24	D	3	100	10-6	0.30	0.5	20	
	F3	2	0.23	0.29	D	3	110	10-6	0.20	0.5	5	
F3	R3	0	0.37	−0.83	D	3	100	10-6	0.50	0.3	24	108–111
	F3	0	0.62	−1.5	D	3	100	10-6	0.50	1	10	119
	L3	0	0.34	−1.5	D	3	100	10-6	0.42	1	10	119
	R3	1	0.3	−0.7	D	3	100	10-6	0.50	0.3	24	
	R3	2	0.24	−0.6	D	3	100	10-6	0.50	0.3	24	
L3	R3	0	0.54	−0.23	D	3	250	10-6	0.32	0.5	24	108, 113, 114, 120–122
	F3	0	0.53	−0.8	D	3	100	10-6	0.53	1	10	109
	L3	0	0.09	−1.5	F	3	600	1000	0.09	1	10	109
	R5	0	0.35	−0.2						1	20	
	F5	0	0.53	−0.83						1	10	
	I5	0	0.04	−0.08						1	20	
	R6	0	0.25	−0.2						1	20	
	F6	0	0.53	−0.5						1	10	
R4	R3	0	0.16	1.25						0.5	15	55, 82, 114, 123
	F3	0	0.23	1						0.1	5	
	L3	0	0.02	0.3						0.1	5	
	R4	0	0.1	1.09						0.8	18	44, 55, 123–127

Table A.1. (*Continued*)

Presynaptic neuron	Possynaptic neuron	Columns away	Connections		Type	STP				PSP		References
			Probability	Strength		T1	Trec	TF	U	T1	T2	
	F4	0	0.55	1.73	D	3	250	10-6	0.26	0.1	7	44, 55, 114, 126
	L4	0	0.26	0.5775	F	3	20	300	0.01	0.5	15	3, 44, 114, 120
	R5	0	0.08	0.53						1	12	44, 128
	F5	0	0.1	0.45						0.1	5	
	I5	0	0.08	0.53						1	12	
	R6	0	0.03	0.25						1	12	
	F6	0	0.01	0.1						0.1	5	
	R4	1	0.08	0.872						0.8	18	
	F4	1	0.44	1.038	D	3	250	10-6	0.26	0.1	7	
	F4	2	0.22	0.623	D	3	250	10-6	0.26	0.1	7	
F4	R4	0	0.35	−1.025	D	3	250	10-6	0.26	0.08	20	44, 114, 126, 129
	F4	0	0.74	−1.5						1	10	
	L4	0	0.36	−1						1	10	
	R4	1	0.28	−0.82	D	3	250	10-6	0.26	0.08	20	
	R4	2	0.22	−0.61	D	3	250	10-6	0.26	0.08	20	
L4	R3	0	0.1	−0.4						1	20	
	F3	0	0.3	−0.4						1	10	
	R4	0	0.39	−0.839	F	2	70	60	0.09	0.3	25	44, 114, 120
	F4	0	0.62	−0.8						1	10	
	L4	0	0.08	−0.8						1	10	
	R5	0	0.1	−0.4						1	20	
	F5	0	0.3	−0.4						1	10	
	R6	0	0.05	−0.2						1	20	
	F6	0	0.15	−0.2						1	10	
R5	R3	0	0.08	0.9	D	3	100	10-6	0.40	1	12	14
	F3	0	0.43	0.86						0.1	5	
	L3	0	0.52	0.5						0.1	5	
	R4	0	0.01	0.48						1	12	
	F4	0	0.43	0.5						0.1	5	
	L4	0	0.51	0.3						0.1	5	
	R5	0	0.087	0.588	D	3	350	10-6	0.50	0.8	15	56, 116, 118, 130–138
	F5	0	0.6	0.585						0.1	12	56, 114, 139
	L5	0	0.08	0.4039						0.1	7	56, 135, 140
	I5	0	0.087	0.588	D	3	350	10-6	0.50	1	12	
	R6	0	0.03	0.5						1	12	
	F6	0	0.1	0.05						0.1	5	
	L6	0	0.19	0.02						0.1	5	
	R5	1	0.066	0.47	D	3	350	10-6	0.50	0.8	15	
	F5	1	0.275	0.4						0.1	12	
	I5	1	0.07	0.47	D	3	350	10-6	0.50	1	12	
	R5	2	0.049	0.376	D	3	350	10-6	0.50	0.8	15	
	F5	2	0.2	0.17						0.1	12	
	I5	2	0.056	0.376	D	3	350	10-6	0.50	1	12	
F5	R5	0	0.33	−0.8	D	3	60	10-6	0.60	1	15	14, 55, 114, 141
	F5	0	0.62	−1.5	D	3	80	10-6	0.50	1	10	142
	L5	0	0.34	−1						1	10	
	I5	0	0.1	−0.8	D	3	60	10-6	0.60	1	15	
	R5	1	0.26	−0.64	D	3	60	10-6	0.60	1	15	
	I5	1	0.06	−0.4	D	3	60	10-6	0.60	1	15	

Table A.1. (*Continued*)

Presynaptic neuron	Possynaptic neuron	Columns away	Connections		Type	STP				PSP		References
			Probability	Strength		T1	Trec	TF	U	T1	T2	
	R5	2	0.21	−0.51	D	3	60	10-6	0.60	1	15	
	I5	2	0.03	−0.2	D	3	60	10-6	0.60	1	15	
L5	R3	0	0.35	−0.83						1	20	
	F3	0	0.53	−0.83						1	10	
	R5	0	0.35	−0.83						1	20	14
	F5	0	0.53	−1						1	10	
	L5	0	0.09	−1						1	10	
	I5	0	0.03	−0.08						1	20	
	R6	0	0.25	−0.83						1	20	
	F6	0	0.53	−0.83						1	10	
I5	R3	0	0.08	0.9	D	3	100	10-6	0.4	1	12	
	F3	0	0.43	0.5						0.1	5	
	L3	0	0.52	0.3						0.1	5	
	R4	0	0.01	0.48						1	12	
	F4	0	0.43	0.5						0.1	5	
	L4	0	0.51	0.3						0.1	5	
	R5	0	0.176	0.7	D	3	350	10-6	0.5	1	12	
	F5	0	0.25	0.56						0.1	5	
	L5	0	0.08	0.62						0.1	5	
	I5	0	0.16	1.06						1	12	
	R6	0	0.03	0.6						1	12	
	F6	0	0.1	0.05						0.1	5	
	L6	0	0.19	0.02						0.1	5	
	R3	1	0.04	0.45	D	3	100	10-6	0.40	1	12	
	F3	1	0.21	0.43						0.1	5	
	L3	1	0.25	0.25						0.1	5	
	R5	1	0.15	0.8	D	3	350	10-6	0.5	1	12	
	F5	1	0.15	0.4						0.1	5	
	L5	1	0.06	0.5						0.1	5	
	I5	1	0.112	0.8	D	3	350	10-6	0.5	1	12	
	R3	2	0.02	0.23	D	3	100	10-6	0.4	1	12	
	F3	2	0.09	0.22						0.1	5	
	L3	2	0.13	0.13						0.1	5	
	R5	2	0.06	0.5	D	3	350	10-6	0.5	1	12	
	F5	2	0.032	0.3						0.1	5	
	L5	2	0.05	0.4						0.1	5	
	I5	2	0.078	0.2	D	3	350	10-6	0.5	1	12	
R6	R4	0	0.002	0.23						0.1	15	126
	F4	0	0.05	0.34						0.01	3	
	R5	0	0.018	1.39						0.8	20	143
	F5	0	0.15	0.51						0.1	5	
	I5	0	0.018	1.39						1	12	
	R6	0	0.036	0.5	D	3	150	10-6	0.2	0.8	10	47, 143
	F6	0	0.225	0.69	F	2	70	100	0.1	0.1	7	47, 143
	L6	0	0.21	0.16						1	7	143
	F6	1	0.18	0.28	F	2	70	100	0.1	0.1	7	
	F6	2	0.14	0.11	F	2	70	100	0.1	0.1	7	
F6	R6	0	0.44	−0.9						1	15	
	F6	0	0.62	−1.5						1	10	

Table A.1. (*Continued*)

Presynaptic neuron	Possynaptic neuron	Columns away	Connections		Type	STP				PSP		References
			Probability	Strength		T1	Trec	TF	U	T1	T2	
	L6	0	0.34	−1						1	10	
	R6	1	0.35	−0.72						1	15	
	L6	2	0.28	−0.57						1	10	
L6	R3	0	0.35	−0.83						1	20	
	F3	0	0.53	−0.83						1	10	
	R5	0	0.25	−0.83						1	20	
	F5	0	0.53	−0.83						1	10	
	I5	0	0.25	−0.83						1	20	
	R6	0	0.35	−0.63						1	20	
	F6	0	0.53	−0.83						1	10	
	L6	0	0.09	−0.63						1	10	

percentage of the values obtained for the same connection within a column. The percentage is cell-type specific and is based on the references cited for connections within a column.

References

1. R. J. Douglas and K. A. Martin, Neuronal circuits of the neocortex, *Annu. Rev. Neurosci.* **27** (2004) 419–451.
2. A. J. Trevelyan, D. Sussillo, B. O. Watson and R. Yuste, Modular propagation of epileptiform activity: Evidence for an inhibitory veto in neocortex, *J. Neurosci.* **26** (2006) 12447–12455.
3. A. M. Thomson and D. C. West, Presynaptic frequency filtering in the gamma frequency band; dual intracellular recordings in slices of adult rat and cat neocortex, *Cereb. Cortex* **13** (2003) 136–143.
4. Y. Kubota and Y. Kawaguchi, Three classes of GABAergic interneurons in neocortex and neostriatum, *Jpn. J. Physiol.* **44 Suppl 2** (1994) S145–S148.
5. J. L. Ramirez *et al.*, Deficiency of somatostatin (SST) receptor type 5 (SSTR5) is associated with sexually dimorphic changes in the expression of SST and SST receptors in brain and pancreas, *Mol. Cell Endocrinol.* **221** (2004) 105–119.
6. Y. Wang *et al.*, Anatomical, physiological and molecular properties of Martinotti cells in the somatosensory cortex of the juvenile rat, *J. Physiol.* **561** (2004) 65–90.
7. Y. Kawaguchi and Y. Kubota, Physiological and morphological identification of somatostatin- or vasoactive intestinal polypeptide-containing cells among GABAergic cell subtypes in rat frontal cortex, *J. Neurosci.* **16** (1996) 2701–2715.
8. Y. Kawaguchi and S. Kondo, Parvalbumin, somatostatin and cholecystokinin as chemical markers for specific GABAergic interneuron types in the rat frontal cortex, *J. Neurocytol.* **31** (2002) 277–287.
9. H. Monyer and H. Markram, Interneuron diversity series: Molecular and genetic tools to study GABAergic interneuron diversity and function, *Trends Neurosci.* **27** (2004) 90–97.
10. A. Bacci, U. Rudolph, J. R. Huguenard and D. A. Prince, Major differences in inhibitory synaptic transmission onto two neocortical interneuron subclasses, *J. Neurosci.* **23** (2003) 9664–9674.
11. A. Bacci, J. R. Huguenard and D. A. Prince, Modulation of neocortical interneurons: Extrinsic influences and exercises in self-control, *Trends Neurosci.* **28** (2005) 602–610.
12. Y. Kawaguchi, Physiological, morphological, and histochemical characterization of three classes of interneurons in rat neostriatum, *J. Neurosci.* **13** (1993) 4908–4923.
13. Y. Kubota and Y. Kawaguchi, Two distinct subgroups of cholecystokinin-immunoreactive cortical interneurons, *Brain Res.* **752** (1997) 175–183.
14. A. M. Thomson, D. C. West, J. Hahn and J. Deuchars, Single axon IPSPs elicited in pyramidal cells by three classes of interneurones in slices of rat neocortex, *J. Physiol.* **496**(Pt 1) (1996) 81–102.
15. A. Binaschi, G. Bregola and M. Simonato, On the role of somatostatin in seizure control: Clues from the hippocampus, *Rev. Neurosci.* **14** (2003) 285–301.
16. R. J. Robbins *et al.*, A selective loss of somatostatin in the hippocampus of patients with temporal lobe epilepsy, *Ann. Neurol.* **29** (1991) 325–332.
17. R. Kuruba, B. Hattiangady, V. K. Parihar, B. Shuai and A. K. Shetty, Differential susceptibility of interneurons expressing neuropeptide Y or parvalbumin in the aged hippocampus to acute seizure activity, *PLoS One* **6** (2011) e24493.
18. P. R. Hof *et al.*, Age-related changes in GluR2 and NMDAR1 glutamate receptor subunit protein

immunoreactivity in corticocortically projecting neurons in macaque and patas monkeys, *Brain Res.* **928** (1991) 175–186.
19. R. Miettinen *et al.*, Neocortical, hippocampal and septal parvalbumin- and somatostatin-containing neurons in young and aged rats: Correlation with passive avoidance and water maze performance, *Neuroscience* **53** (1993) 367–378.
20. S. A. Trotter, J. Kapur, M. J. Anzivino and K. S. Lee, GABAergic synaptic inhibition is reduced before seizure onset in a genetic model of cortical malformation, *J. Neurosci.* **26** (2006) 10756–10767.
21. P. J. Franaszczuk, P. Kudela and G. K. Bergey, External excitatory stimuli can terminate bursting in neural network models, *Epilepsy Res.* **53** (2003) 65–80.
22. E. M. Izhikevich, Which model to use for cortical spiking neurons? *IEEE Trans. Neural Netw.* **15** (2004) 1063–1070.
23. J. J. Lovelace and K. J. Cios, A very simple spiking neuron model that allows for modeling of large, complex systems (2007), Available at <http://www.mitpressjournals.org/doi/abs/10.1162/neco.2008.20.1.65>.
24. W. Gerstner, A. K. Kreiter, H. Markram and A. V. Herz, Neural codes: Firing rates and beyond, *Proc. Natl. Acad. Sci. U. S. A.* **94** (1997) 12740–12741.
25. R. D. Traub *et al.*, Single-column thalamocortical network model exhibiting gamma oscillations, sleep spindles, and epileptogenic bursts, *J. Neurophysiol.* **93** (2005) 2194–2232.
26. W. W. Lytton, Computer modelling of epilepsy, *Nat. Rev. Neurosci.* **9** (2008) 626–637.
27. J.-M. Fellous, Regulation of persistent activity by background inhibition in an *in vitro* model of a cortical microcircuit, *Cereb. Cortex* **13** (2003) 1232–1241.
28. F. Wendling, Computational models of epileptic activity: A bridge between observation and pathophysiological interpretation, *Expert Rev. Neurother.* **8** (2008) 889–896.
29. G. Deco , V. K. Jirsa, P. A. Robinson, M. Breakspear and K. Friston, The Dynamic Brain: From Spiking Neurons to Neural Masses and Cortical Fields, *PLoS Comput Biol* **4** (2008) e1000092.
30. P. Suffczynski, S. Kalitzin and F. H. Lopes da Silva, Dynamics of non-convulsive epileptic phenomena modeled by a bistable neuronal network, *Neuroscience* **126** (2004) 467–484.
31. S. Ghosh-Dastidar and H. Adeli, Improved spiking neural networks for EEG classification and epilepsy and seizure detection, *Integr. Comput. Aided. Eng.* **14** (2007) 187–212.
32. H. Lim *et al.*, Connectional parameters determine multisensory processing in a spiking network model of multisensory convergence, *Exp. Brain Res.* **213** (2011) 329–339.
33. R. D. Traub, J. G. Jefferys and M. A. Whittington, Simulation of gamma rhythms in networks of interneurons and pyramidal cells, *J. Comput. Neurosci.* **4** (1997) 141–50.
34. P. Bush and T. Sejnowski, Inhibition synchronizes sparsely connected cortical neurons within and between columns in realistic network models, *J. Comput. Neurosci.* **3** (1996) 91–110.
35. R. D. Traub *et al.*, GABA-enhanced collective behavior in neuronal axons underlies persistent gamma-frequency oscillations, *Proc. Natl. Acad. Sci. U. S. A.* **100** (2003) 11047–11052.
36. M. A. Whittington, R. D. Traub, N. Kopell, B. Ermentrout and E. H. Buhl, Inhibition-based rhythms: Experimental and mathematical observations on network dynamics, *Int. J. Psychophysiol.* **38** (2000) 315–336.
37. C. Börgers, S. Epstein and N. J. Kopell, Background gamma rhythmicity and attention in cortical local circuits: A computational study, *Proc. Natl. Acad. Sci. U. S. A.* **102** (2005) 7002–7007.
38. M. O. Cunningham *et al.*, A role for fast rhythmic bursting neurons in cortical gamma oscillations *in vitro*, *Proc. Natl. Acad. Sci. U. S. A.* **101** (2004) 7152–7157.
39. T. Yamanishi, J.-Q. Liu and H. Nishimura, Modeling fluctuations in default-mode brain network using a spiking neural network, *Int. J. Neural Syst.* **22** (2012) 1250016.
40. E. M. E. Izhikevich and G. G. M. Edelman, Large-scale model of mammalian thalamocortical systems, *Proc. Natl. Acad. Sci. U. S. A.* **105** (2008) 3593–3598.
41. H. Markram, The blue brain project, *Nat. Rev. Neurosci.* **7** (2006) 153–160.
42. P. Suffczynski, S. Kalitzin, G. Pfurtscheller and F. H. Lopes da Silva, Computational model of thalamo-cortical networks: Dynamical control of alpha rhythms in relation to focal attention, *Int. J. Psychophysiol.* **43** (2001) 25–40.
43. A. L. George and K. M. Jacobs, Altered intrinsic properties of neuronal subtypes in malformed epileptogenic cortex, *Brain Res.* **1374** (2011) 116–128.
44. M. Beierlein, J. R. Gibson and B. W. Connors, Two dynamically distinct inhibitory networks in layer 4 of the neocortex, *J. Neurophysiol.* **90** (2003) 2987–3000.
45. A. M. Thomson and C. Lamy, Functional maps of neocortical local circuitry, *Frontiers in Neuroscience* **1**(2) (2007) 19–42.
46. S. Lefort, C. Tomm, J. C. Floyd Sarria and C. C. Petersen, The excitatory neuronal network of the C2 barrel column in mouse primary somatosensory cortex, *Neuron* **61** (2009) 301–316.
47. M. Beierlein and B. W. Connors, Short-term dynamics of thalamocortical and intracortical

synapses onto layer 6 neurons in neocortex, *J. Neurophysiol.* **88** (2002) 1924–1932.
48. D. Goodman and R. Brette, Brian: A simulator for spiking neural networks in python, *Front. Neuroinform.* **2** (2008) 5.
49. M.-O. Gewaltig and M. Diesmann, NEST (Neural Simulation Tool), *Scholarpedia* **2** (2007) 1430.
50. E. Ros, R. Carrillo, E. M. Ortigosa, B. Barbour and R. Agís, Event-driven simulation scheme for spiking neural networks using lookup tables to characterize neuronal dynamics, *Neural Comput.* **18** (2006) 2959–2993.
51. R. Brette *et al.*, Simulation of networks of spiking neurons: A review of tools and strategies, *J. Comput. Neurosci.* **23** (2007) 349–398.
52. B. W. Connors and A. E. Telfeian, Dynamic properties of cells, synapses, circuits, and seizures in neocortex, *Adv. Neurol.* **84** (2000) 141–152.
53. J. Lubke and D. Feldmeyer, Excitatory signal flow and connectivity in a cortical column: Focus on barrel cortex, *Brain Struct. Funct.* **212** (2007) 3–17.
54. H. Markram *et al.*, Interneurons of the neocortical inhibitory system, *Nat. Rev. Neurosci.* **5** (2004) 793–807.
55. A. M. Thomson, D. C. West, Y. Wang and A. P. Bannister, Synaptic connections and small circuits involving excitatory and inhibitory neurons in layers 2–5 of adult rat and cat neocortex: Triple intracellular recordings and biocytin labelling in vitro, *Cereb. Cortex* **12** (2002) 936–953.
56. A. M. Thomson and J. Deuchars, Synaptic interactions in neocortical local circuits: Dual intracellular recordings *in vitro*, *Cereb. Cortex* **7** (1997) 510–522.
57. J. Watts and A. M. Thomson, Excitatory and inhibitory connections show selectivity in the neocortex, *J. Physiol.* **562** (2005) 89–97.
58. N. Voges, A. Schüz, A. Aertsen and S. Rotter, A modeler's view on the spatial structure of intrinsic horizontal connectivity in the neocortex, *Prog. Neurobiol.* **92** (2010) 277–292.
59. J. DeFelipe *et al.*, Neocortical circuits: Evolutionary aspects and specificity versus non-specificity of synaptic connections. Remarks, main conclusions and general comments and discussion, *J. Neurocytol.* **31** (2002) 387–416.
60. J. Q. Ren, Y. Aika, C. W. Heizmann and T. Kosaka, Quantitative analysis of neurons and glial cells in the rat somatosensory cortex, with special reference to GABAergic neurons and parvalbumin-containing neurons, *Exp. Brain Res.* **92** (1992) 1–14.
61. K. Mizukawa, P. L. McGeer, S. R. Vincent and E. G. McGeer, The distribution of somatostatin-immunoreactive neurons and fibers in the rat cerebral cortex: Light and electron microscopic studies, *Brain Res.* **426** (1987) 28–36.
62. B. W. Connors, M. J. Gutnick and D. A. Prince, Electrophysiological properties of neocortical neurons *in vitro*, *J. Neurophysiol.* **48** (1982) 1302–1320.
63. B. W. Connors and M. J. Gutnick, Intrinsic firing patterns of diverse neocortical neurons, *Trends Neurosci.* **13** (1990) 99–104.
64. D. Cosandier-Rimélé, I. Merlet, F. Bartolomei, J.-M. Badier and F. Wendling, Computational modeling of epileptic activity: From cortical sources to EEG signals, *J. Clin. Neurophysiol.* **27** (2010) 465–470.
65. E. M. Izhikevich, Simple model of spiking neurons, *IEEE Trans. Neural Netw.* **14** (2003) 1569–1572.
66. E. M. Izhikevich, *Dynamical Systems in Neuroscience* (MIT Press, 2007), p. 441.
67. B. Strack, K. M. Jacobs and K. J. Cios, Biological restraint on the Izhikevich neuron model essential for seizure modeling, in *Neural Eng. 2013. Conf. Proc. 6th Annu. Int. IEEE EMBS Conf.* (2013), pp. 395–398.
68. G. Deco, V. K. Jirsa, P. A. Robinson, M. Breakspear and K. Friston, The dynamic brain: From spiking neurons to neural masses and cortical fields, *PLoS Comput. Biol.* **4** (2008) e1000092.
69. A. Roxin, N. Brunel, D. Hansel, G. Mongillo and C. van Vreeswijk, On the distribution of firing rates in networks of cortical neurons, *J. Neurosci.* **31** (2011) 16217–16226.
70. M. Tsodyks, A. Uziel and H. Markram, Synchrony generation in recurrent networks with frequency-dependent synapses, *J. Neurosci.* **20** (2000) RC50.
71. M. Gilson, A. N. Burkitt, D. B. Grayden, D. A. Thomas and J. L. van Hemmen, Emergence of network structure due to spike-timing-dependent plasticity in recurrent neuronal networks IV: Structuring synaptic pathways among recurrent connections, *Biol. Cybern.* **101** (2009) 427–444.
72. R. Legenstein, H. Markram and W. Maass, Input prediction and autonomous movement analysis in recurrent circuits of spiking neurons, *Rev. Neurosci.* **14** (2003) 5–19.
73. M. J. Richardson, O. Melamed, G. Silberberg, W. Gerstner and H. Markram, Short-term synaptic plasticity orchestrates the response of pyramidal cells and interneurons to population bursts, *J. Comput. Neurosci.* **18** (2005) 323–331.
74. D. Sussillo, T. Toyoizumi and W. Maass, Self-tuning of neural circuits through short-term synaptic plasticity, *J. Neurophysiol.* **97** (2007) 4079–4095.
75. L. F. Abbott and S. B. Nelson, Synaptic plasticity: Taming the beast, *Nat. Neurosci.* **3** (2000) 1178–1183.
76. W. K. Wong, Z. Wang, B. Zhen and S. Leung, Relationship between applicability of current-based synapses and uniformity of firing patterns, *Int. J. Neural Syst.* **22** (2012) 1250017.

77. A. Morrison, M. Diesmann and W. Gerstner, Phenomenological models of synaptic plasticity based on spike timing, *Biol. Cybern.* **98** (2008) 459–478.
78. K. Ramanathan *et al.*, Presynaptic learning and memory with a persistent firing neuron and a habituating synapse: A model of short term persistent habituation, *Int. J. Neural Syst.* **22** (2012) 1250015.
79. M. Tsodyks, K. Pawelzik and H. Markram, Neural networks with dynamic synapses, *Neural Comput.* **10** (1998) 821–835.
80. L. F. Abbott, J. A. Varela, K. Sen and S. B. Nelson, Synaptic depression and cortical gain control, *Science* **275** (1997) 220–224.
81. D. Feldmeyer, J. Lübke, B. Sakmann and J. Lubke, Efficacy and connectivity of intracolumnar pairs of layer 2/3 pyramidal cells in the barrel cortex of juvenile rats, *J. Physiol.* **575** (2006) 583–602.
82. P. Kudela, P. J. Franszczuk and G. K. Bergey, Synaptic plasticity in neuronal network models can explain patterns of bursting activity seen in temporal lobe epileptic seizures, *Conf. Proc. IEEE Eng. Med. Biol. Soc.*, Vol. 1 (2004), pp. 715–717.
83. J.-M. Fellous and T. J. Sejnowski, Regulation of persistent activity by background inhibition in an *in vitro* model of a cortical microcircuit, *Cereb. Cortex* **13** (2003) 1232–1241.
84. A. L. George and K. M. Jacobs, Altered intrinsic properties of neuronal subtypes in malformed epileptogenic cortex, *Brain Res.* **1374** (2011) 116–128.
85. M. Armstrong-James, K. Fox and A. Das-Gupta, Flow of excitation within rat barrel cortex on striking a single vibrissa, *J. Neurophysiol.* **68** (1992) 1345–1358.
86. M. Beierlein, J. R. Gibson and B. W. Connors, A network of electrically coupled interneurons drives synchronized inhibition in neocortex, *Nat Neurosci.* **3** (2000) 904–910.
87. M. A. Long, S. J. Cruikshank, M. J. Jutras and B. W. Connors, Abrupt maturation of a spike-synchronizing mechanism in neocortex, *J. Neurosci.* **25** (2005) 7309–7316.
88. M. A. Whittington, R. D. Traub and J. G. R. Jefferys, Synchronized oscillations in interneuron networks driven by metabotropic glutamate receptor activation, *Nature* **373** (1995) 612–615.
89. H. P. Robinson and N. Kawai, Single channel properties at the synaptic site, *EXS* **63** (1993) 250–265.
90. L. L. Zhang, P. A. Collier and K. W. Ashwell, Mechanisms in the induction of neuronal heterotopiae following prenatal cytotoxic brain damage, *Neurotoxicol. Teratol.* **17** (1995) 297–311.
91. B. Strack, K. M. Jacobs and K. J. Cios, Simulating lesions in multi-layer, multi-columnar model of neocortex, in *Neural Eng. 2013. Conf. Proc. 6th Annu. Int. IEEE EMBS Conf.* (2013), pp. 835–838.
92. A. E. Telfeian and B. W. Connors, Layer-specific pathways for the horizontal propagation of epileptiform discharges in neocortex, *Epilepsia* **39** (1998) 700–708.
93. Y. Chagnac-Amitai and B. W. Connors, Synchronized excitation and inhibition driven by intrinsically bursting neurons in neocortex, *J. Neurophysiol.* **62** (1989) 1149–1162.
94. Y. Chagnac-Amitai and B. W. Connors, Horizontal spread of synchronized activity in neocortex and its control by GABA-mediated inhibition, *J. Neurophysiol.* **61** (1989) 747–758.
95. B. W. Connors, Initiation of synchronized neuronal bursting in neocortex, *Nature* **310** (1984) 685–687.
96. H. Adeli, Z. Zhou and N. Dadmehr, Analysis of EEG records in an epileptic patient using wavelet transform, *J. Neurosci. Methods* **123** (2003) 69–87.
97. H. Adeli and S. Ghosh-Dastidar, *Automated EEG-Based Diagnosis of Neurological Disorders*: *Inventing the Future of Neurology* (CRC Press, 2010), p. 423.
98. S. Ghosh-Dastidar, H. Adeli and N. Dadmehr, Mixed-band wavelet-chaos-neural network methodology for epilepsy and epileptic seizure detection, *IEEE Trans. Biomed. Eng.* **54** (2007) 1545–1551.
99. H. Adeli, S. Ghosh-Dastidar and N. Dadmehr, A wavelet-chaos methodology for analysis of EEGs and EEG subbands to detect seizure and epilepsy, *IEEE Trans. Biomed. Eng.* **54** (2007) 205–211.
100. K. Vonck *et al.*, A decade of experience with deep brain stimulation for patients with refractory medial temporal lobe epilepsy, *Int. J. Neural Syst.* **23** (2013) 1250034.
101. S. Ghosh-Dastidar and H. Adeli, A new supervised learning algorithm for multiple spiking neural networks with application in epilepsy and seizure detection, *Neural Netw.* **22** (2009) 1419–1431.
102. P. Suffczynski, F. Lopes da Silva, J. Parra, D. Velis and S. Kalitzin, Epileptic transitions: Model predictions and experimental validation, *J. Clin. Neurophysiol.* **22** (2005) 288–299.
103. D. Serletis, P. L. Carlen, T. A. Valiante and B. L. Bardakjian, Phase synchronization of neuronal noise in mouse hippocampal epileptiform dynamics, *Int. J. Neural Syst.* **23** (2013) 1250033.
104. M. O. Cunningham *et al.*, A role for fast rhythmic bursting neurons in cortical gamma oscillations *in vitro*, *Proc. Natl. Acad. Sci. U. S. A.* **101** (2004) 7152–7157.
105. S. Ghosh-Dastidar and H. Adeli, Spiking neural networks, *Int. J. Neural Syst.* **19** (2009) 295–308.
106. A. E. Telfeian and B. W. Connors, Widely integrative properties of layer 5 pyramidal cells support a role for processing of extralaminar synaptic inputs in rat neocortex, *Neurosci. Lett.* **343** (2003) 121–124.

107. R. D. Chervin, P. A. Pierce and B. W. Connors, Periodicity and directionality in the propagation of epileptiform discharges across neocortex, *J. Neurophysiol.* **60** (1988) 1695–1713.
108. C. Kapfer, L. L. Glickfeld, B. V. Atallah and M. Scanziani, Supralinear increase of recurrent inhibition during sparse activity in the somatosensory cortex, *Nat. Neurosci.* **10** (2007) 743–753.
109. A. Reyes *et al.*, Target-cell-specific facilitation and depression in neocortical circuits, *Nat. Neurosci.* **1** (1998) 279–285.
110. C. Holmgren, T. Harkany, B. Svennenfors and Y. Zilberter, Pyramidal cell communication within local networks in layer 2/3 of rat neocortex, *J. Physiol.* **551** (2003) 139–153.
111. M. Blatow *et al.*, A novel network of multipolar bursting interneurons generates theta frequency oscillations in neocortex, *Neuron* **38** (2003) 805–817.
112. J. Von Engelhardt, M. Eliava, A. H. Meyer, A. Rozov and H. Monyer, Functional characterization of intrinsic cholinergic interneurons in the cortex, *J. Neurosci.* **27** (2007) 5633–5642.
113. A. Rozov, J. Jerecic, B. Sakmann and N. Burnashev, AMPA receptor channels with long-lasting desensitization in bipolar interneurons contribute to synaptic depression in a novel feedback circuit in layer 2/3 of rat neocortex, *J. Neurosci.* **21** (2001) 8062–8071.
114. A. B. Ali, A. P. Bannister and A. M. Thomson, Robust correlations between action potential duration and the properties of synaptic connections in layer 4 interneurones in neocortical slices from juvenile rats and adult rat and cat, *J. Physiol.* **580** (2007) 149–169.
115. B. M. Kampa, J. J. Letzkus and G. J. Stuart, Cortical feed-forward networks for binding different streams of sensory information, *Nat. Neurosci.* **9** (2006) 1472–1473.
116. A. M. Thomson and A. P. Bannister, Postsynaptic pyramidal target selection by descending layer III pyramidal axons: Dual intracellular recordings and biocytin filling in slices of rat neocortex, *Neuroscience* **84** (1998) 669–683.
117. N. R. Hardingham *et al.*, Extracellular calcium regulates postsynaptic efficacy through group 1 metabotropic glutamate receptors, *J. Neurosci.* **26** (2006) 6337–6345.
118. A. Reyes and B. Sakmann, Developmental switch in the short-term modification of unitary EPSPs evoked in layer 2/3 and layer 5 pyramidal neurons of rat neocortex, *J. Neurosci.* **19** (1999) 3827–3835.
119. G. Tamás, P. Somogyi and E. H. Buhl, Differentially interconnected networks of GABAergic interneurons in the visual cortex of the cat, *J. Neurosci.* **18** (1998) 4255–4270.
120. G. Tamás, E. H. Buhl and P. Somogyi, Fast IPSPs elicited via multiple synaptic release sites by different types of GABAergic neurone in the cat visual cortex, *J. Physiol.* **500**(Pt 3) (1997) 715–738.
121. M. C. Angulo, J. F. Staiger, J. Rossier and E. Audinat, Developmental synaptic changes increase the range of integrative capabilities of an identified excitatory neocortical connection, *J. Neurosci.* **19** (1999) 1566–1576.
122. E. E. Fanselow, K. A. Richardson and B. W. Connors, Selective, state-dependent activation of somatostatin-expressing inhibitory interneurons in mouse neocortex, *J. Neurophysiol.* **100** (2008) 2640–2652.
123. A. P. Bannister and A. M. Thomson, Dynamic properties of excitatory synaptic connections involving layer 4 pyramidal cells in adult rat and cat neocortex, *Cereb. Cortex* **17** (2007) 2190–2203.
124. D. Feldmeyer, V. Egger, J. Lubke and B. Sakmann, Reliable synaptic connections between pairs of excitatory layer 4 neurones within a single "barrel" of developing rat somatosensory cortex, *J. Physiol.* **521**(Pt 1) (1999) 169–190.
125. A. Maffei, S. B. Nelson and G. G. Turrigiano, Selective reconfiguration of layer 4 visual cortical circuitry by visual deprivation, *Nat. Neurosci.* **7** (2004) 1353–1359.
126. K. Tarczy-Hornoch, K. A. Martin, J. J. Jack and K. J. Stratford, Synaptic interactions between smooth and spiny neurones in layer 4 of cat visual cortex *in vitro*, *J. Physiol.* **508**(Pt 2) (1998) 351–363.
127. C. C. H. Petersen and B. Sakmann, The excitatory neuronal network of rat layer 4 barrel cortex, *J. Neurosci.* **20** (2000) 7579–7586.
128. D. Feldmeyer, A. Roth and B. Sakmann, Monosynaptic connections between pairs of spiny stellate cells in layer 4 and pyramidal cells in layer 5A indicate that lemniscal and paralemniscal afferent pathways converge in the infragranular somatosensory cortex, *J. Neurosci.* **25** (2005) 3423–3431.
129. Y. Wang, A. Gupta, M. Toledo-Rodriguez, C. Z. Wu and H. Markram, Anatomical, physiological, molecular and circuit properties of nest basket cells in the developing somatosensory cortex, *Cereb. Cortex* **12** (2002) 395–410.
130. A. B. Ali, Involvement of post-synaptic kainate receptors during synaptic transmission between unitary connections in rat neocortex, *Eur. J. Neurosci.* **17** (2003) 2344–2350.
131. A. Frick, D. Feldmeyer and B. Sakmann, Postnatal development of synaptic transmission in local networks of L5A pyramidal neurons in rat somatosensory cortex, *J. Physiol.* **585** (2007) 103–116.
132. H. Markram, J. Lübke, M. Frotscher, A. Roth and B. Sakmann, Physiology and anatomy of synaptic

connections between thick tufted pyramidal neurones in the developing rat neocortex, *J. Physiol.* **500**(Pt 2) (1997) 409–440.
133. A. M. Thomson, J. Deuchars and D. C. West, Large, deep layer pyramid-pyramid single axon EPSPs in slices of rat motor cortex display paired pulse and frequency-dependent depression, mediated presynaptically and self-facilitation, mediated postsynaptically, *J. Neurophysiol.* **70** (1993) 2354–2369.
134. Y. Wang *et al.*, Heterogeneity in the pyramidal network of the medial prefrontal cortex, *Nat. Neurosci.* **9** (2006) 534–542.
135. J.-V. Le Bé, G. Silberberg, Y. Wang and H. Markram, Morphological, electrophysiological, and synaptic properties of corticocallosal pyramidal cells in the neonatal rat neocortex, *Cereb. Cortex* **17** (2007) 2204–2213.
136. N. Kalisman, G. Silberberg and H. Markram, The neocortical microcircuit as a tabula rasa, *Proc. Natl. Acad. Sci. U. S. A.* **102** (2005) 880–885.
137. Z. Gil and Y. Amitai, Properties of convergent thalamocortical and intracortical synaptic potentials in single neurons of neocortex, *J. Neurosci.* **16** (1996) 6567–6578.
138. N. R. Hardingham *et al.*, Quantal analysis reveals a functional correlation between presynaptic and postsynaptic efficacy in excitatory connections from rat neocortex, *J. Neurosci.* **30** (2010) 1441–1451.
139. M. C. Angulo, J. Rossier and E. Audinat, Postsynaptic glutamate receptors and integrative properties of fast-spiking interneurons in the rat neocortex, *J. Neurophysiol.* **82** (1999) 1295–1302.
140. A. M. Thomson, D. C. West and J. Deuchars, Properties of single axon excitatory postsynaptic potentials elicited in spiny interneurons by action potentials in pyramidal neurons in slices of rat neocortex, *Neuroscience* **69** (1995) 727–738.
141. G. Silberberg and H. Markram, Disynaptic inhibition between neocortical pyramidal cells mediated by Martinotti cells, *Neuron* **53** (2007) 735–746.
142. S. Pangratz-Fuehrer and S. Hestrin, Synaptogenesis of electrical and GABAergic synapses of fast-spiking inhibitory neurons in the neocortex, *J. Neurosci.* **31** (2011) 10767–10775.
143. D. C. West, A. Mercer, S. Kirchhecker, O. T. Morris and A. M. Thomson, Layer 6 cortico-thalamic pyramidal cells preferentially innervate interneurons and generate facilitating ePSPs, *Cereb. Cortex.*